Detection of Bitter Limonin in Citrus Samples Using Plasmonic Gold Nanobipyramid-Based Dual-Mode Lateral Flow Immunoassay

Tian Zhang [a,b,c], *Chenxi Guo* [a,b,c], *Lu Yang* [a,b,c], *Lei Liu* [a,b,c], *Di Sun* [a,b,c], *Xinqi Long* [a,b,c], *Qi Wu* [a,b,c], *Qiyang Zhao* [a,b,c], *Yaohai Zhang* [a,b,c], *Jing Li* [a,b,c], *Yongliang Cui* [*, a,b,c], *Yue He* [*,a,b,c]

[a] *Key Laboratory of Quality and Safety Control of Citrus Fruits, Ministry of Agriculture and Rural Affairs, Southwest University, Chongqing, 400712, P.R. China;*

[b] *Laboratory of Quality & Safety Risk Assessment for Citrus Products (Chongqing), Ministry of Agriculture and Rural Affairs, Citrus Research Institute, Southwest University, Chongqing, 400712, P.R. China;*

[c] *National Citrus Engineering Research Center, Chongqing, 400712, P.R. China*

* To whom correspondence should be addressed. Tel: 86-23-68349603, Fax: 86-23-68349046, Dr. Yue He, E-mail: yhe@swu.edu.cn; Yongliang Cui, E-mail: cuiyongliang@cric.cn

This file contains:

1. Supporting apparatus, materials, reagents, and experiments

2. Supporting figures 1- 7 with legends

3. Supporting table 1-3

1. Supporting apparatus and experiments

1.1 Synthesis of limonin hapten

Using our previously reported method[1], the details are as follows: Limonin (0.20 g, 0.42 mmol), carboxymethoxylamine hemihydrochloride (CMO) (0.20 g, 1.83 mmol) and 5 mL pyridine were added to the reaction bottle. After heating and refluxing for 24 h, the reaction mixture was poured into 20 mL of water. Then, hydrochloric acid (HCl) was added to adjust the pH to 3. Next, ethyl acetate (75 mL) was used to extract the reaction solution for a total of three times. Anhydrous $MgSO_4$ was added into the organic phase and allowed to stand for 1 h. The filtered solution was concentrated under reduced pressure. After that, purified limonin hapten can be obtained through silica gel chromatography.

1.2 Preparation of limonin coating antigen (BSA-limonin) and monoclonal antibody (mAb)

Using our previously reported method [1], the details are as follows: On the basis of the active ester method, the synthesized limonin hapten was combined with bovine serum albumin (BSA), ovalbumin (OVA). The detailed operations were as follows. First of all, limonin hapten (15 mg, 0.028 mmol) was added into N, N-dimethylformamide (DMF) (1 mL) which N-hydroxysuccinimide (NHS) (4.76 mg, 0.041 mmol) and dicyclohexylcarbodiimide (DCC) (6.19 mg, 0.030 mmol) had already been dissolved in before. Then, after stirring for 6 h at 25 ℃, the reaction was centrifuged to remove the precipitate. Divided the supernatant into two parts, and then added them drop-wise into 5 mL of phosphate-buffered saline (PBS), in which 30 mg

of BSA (or 20 mg of OVA) had been dissolved. After reacting at 4 ℃ for 18 h, the mixture was dialyzed with PBS. Subsequently, the solution was dialyzed with PBS for 3 days. Lastly, the fully dialyzed reaction product solution was stored at －80 ℃.

For the preparation of mAb, the animal immunization procedures used in this study are as follows. During the initial immunization, 1 mL of BSA-limonin was absorbed with a sterile injection syringe and added into a sterile glass bottle, and 1 mL of complete Freund's adjuvant was added at the same time, and then quickly mixed under ice bath conditions to fully emulsify. A total of six Balb/c mice were immunized and 100 μg of emulsified antigen was injected into each mouse (50 μg was injected intraperitoneally, 50 μg was injected subcutaneously). After two weeks, incomplete Freund's adjuvant was used for emulsification, and then the second immunization was carried out according to the above process. Next, the mice were immunized once every fifteen days in the same way. After five immunizations, orbital blood was collected for assay. According to checkerboard titration, mouse serum titers were detected to screen out the mice with the best immune performance. Myeloma cells Sp2/0 were resuscitated one week and subcultured before fusion and the mouse with best immune performance was injected 100 μg BSA-limonin without adjuvant three days before cell fusion. After that, spleen cells were collected from the selected mouse and fused with myeloma cells at the ratio of spleen cells to myeloma cells of 10:1 using PEG-2000. After 10 days of cell culture in hypoxanthineaminopterin-thymidin (HAT) medium dulbecco modified eagle medium (DMEM) supplemented with 20% fetal bovine serum (FBS) (v/v), 0.2 M Lglutamine, 50000 U/L penicillin, 50 mg/L streptomycin, 1% HAT (v/ v)), the cell

supernatant was detected by indirect competitive enzyme-linked immunosorbent assay (icELISA). The hybridoma cells with high titer and inhibition were selected, and then the monoclonal cell strains were obtained by limiting dilution and expanded to guarantee monoclonality. Paraffin was injected into the abdominal cavity of mice, and the cultured monoclonal hybridoma cells were intraperitoneally injected into mice one week later. After 7-10 days, the producing ascites were collected and stored at －80 ℃.

1.3 Preparation of gold seeds and gold nanobipyramid (AuNBP)

Refer to Sánchez-Iglesias et al.'s method for preparing gold seeds and AuNBP [2], the details are as follows: Initial gold seeds were prepared in a scintillation vial (20 mL) by fast reduction of chloroauric acid ($HAuCl_4$) (8 mL, 0.313 mM) with freshly prepared Sodium borohydride ($NaBH_4$) (0.25 mL, 250 mM) in an aqueous hexadecyltrimethylammonium chloride (CTAC) solution (1mL,500 mM), in the presence of sodium citrate (1mL, 50 mM) under vigorous stirring 2 min at room temperature. The mixture turned from light yellow to brownish indicating the formation of gold seeds. After 2 min, the vial was closed and the seed solution was heated in an oil bath at 80 ºC for 90 min under gentle stirring, leading to a gradual color change from brown to red. Finally, the thermally treated seed solution was removed from the bath and stored at room temperature. The final Au concentration in the seed solution was 78.4 mM.

A certain volume of gold seeds (0.12 mL, 0,25 mM) was added under vigorous stirring to an aqueous growth solution containing, $HAuCl_4$ (0.6 mL, 10 mM), $AgNO_3$

(0.2 mL, 10 mM), hexadecyltrimethylammonium bromide (CTAB) (20 mL, 100 mM), (HCl) (0.4 mL, 1M) and ascorbic acid (AA) (0.17 mL, 50 mM). The mixture was kept at 30 °C for 2 h.

1.4 Photothermal conversion of AuNBP and AuNBP@ mAb

The photothermal efficiency of AuNBP and AuNBP@ mAb were evaluated using a commercially available 808 nm laser operated at a power density of 2 W·cm^{-2}. Firstly, the prepared AuNBP and AuNBP@ mAb were exposed to near-infrared (NIR) light for 10 min. Temperature data and photothermal images were gathered at each time point. Then the photothermal conversion of AuNBP and AuNBP@ mAb were investigated via temperature elevation after 10 min of NIR laser irradiation. Specifically, when the temperature reached the peak, we turned off the laser and cooled the solution for 10 min. This process was repeated 5 times. The temperature was recorded at each time point.

Subsequently, the dimensionless drive force temperature θ was determined using the recorded temperature (T) through equation (1):

$$\theta = (T - T_{sur})/(T_{max} - T_{sur}) \quad (1)$$

where T_{max} and T_{sur} are the maximum steady-state temperature and the surrounding temperature, respectively. Then, the cooling time (t) was plotted with the negative natural logarithm of θ. The heat transfer time constant (τ_s) is exactly the slope of the fitted line:

$$t = -\tau_s ln\theta \quad (2)$$

After determining τ_s, we calculated hS as follows:

$$hS = m_i C_{p,j}/\tau_s \quad (3)$$

where h is the heat transfer coefficient, S is the surface area of the container, m_i is the mass of the AuNBPor AuNBP@ mAb (1 g), and $C_{p,j}$ represents the heat capacity of the solution (4.2 J/(g.°C). Here, we used the value of water to approximate substitution.

At the same time, the input heat energy due to light absorption by the solvent was calculated as follows:

$$Qdis = \sum_i m_i C_{p,j}(T_{max} - T_{sur})/t \quad (4)$$

where t is the time needed by the solvent to reach maximum temperature difference.

Finally, we calculated the photothermal conversion efficiency (η) of AuNBP and AuNBP@ mAb:

$$\eta = \left[hS(T_{max} - T_{sur}) - Q_{dis}\right]/I(1 - 10^{-A_\lambda}) \quad (5)$$

where I is the laser power (2 W), and A_λ is the absorbance intensity of AuNBP or AuNBP@ mAb at 757 nm.

1.5 Detection of limonin using UPLC-MS/MS

Firstly, the methanol extract was filtrated through a membrane with a pore size of 0.2 μm in order to eliminate impurities. Agilent eclipse plus C18 column from Agilent was used here. The column temperature and injection volume were 40 ℃ and 3 μL, respectively. Pumping of the mobile phase, which included 0.1 percent v/v formic acid in water (A) and methanol (B), took place at a rate of 0.3 mL/min. A linear mobile phase gradient began with 90% A (0.00–0.20 min), decreased to 10% A (0.20–4.00

min) and decreased to 2% A (4.00–6.00 min) and maintained at 2 % A (6.00–8.00 min), followed by 1 min of column balancing at 90% A. The MS meter equipped with a triple quadrupole detector was run in AJS ESI+ source and MRM mode. Two ions were chosen, with the stronger transition (471.3/161.2) used for quantification and the other one (471.3/425.4) for verification. The MS conditions were: nozzle voltage of 500 V, source at 200 °C, sheath gas at 375 °C, 12 L/min sheath gas flow, 14 L/min gas flow, collision gas pressure of 20 psi, and capillary voltage of 3000 V.

2. Supporting figures 1- 7 with legends

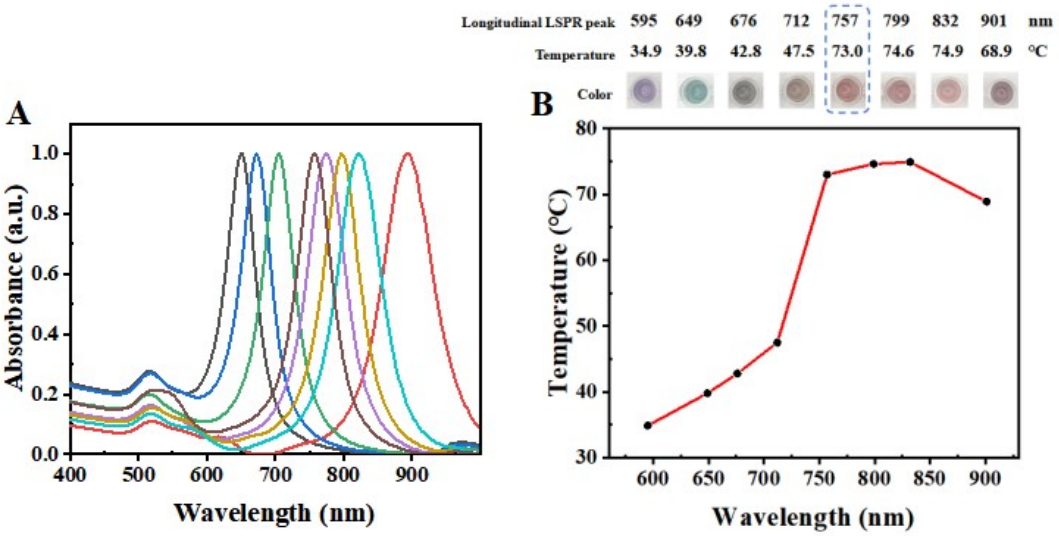

Figure S1. (A) Ultraviolet–visible (UV-Vis) absorption spectra of AuNBP with varying longitudinal LSPR peaks. (B) Temperature variation of AuNBP with varying longitudinal LSPR peaks after 1 minute of NIR laser irradiation. Inset: Corresponding temperature and color images.

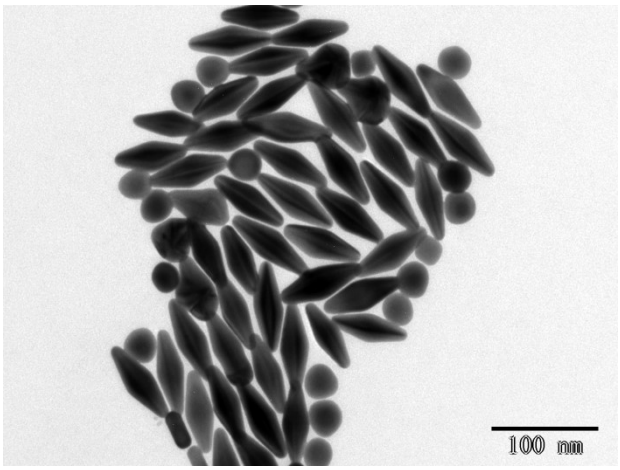

Figure S2. TEM image of AuNBP. .

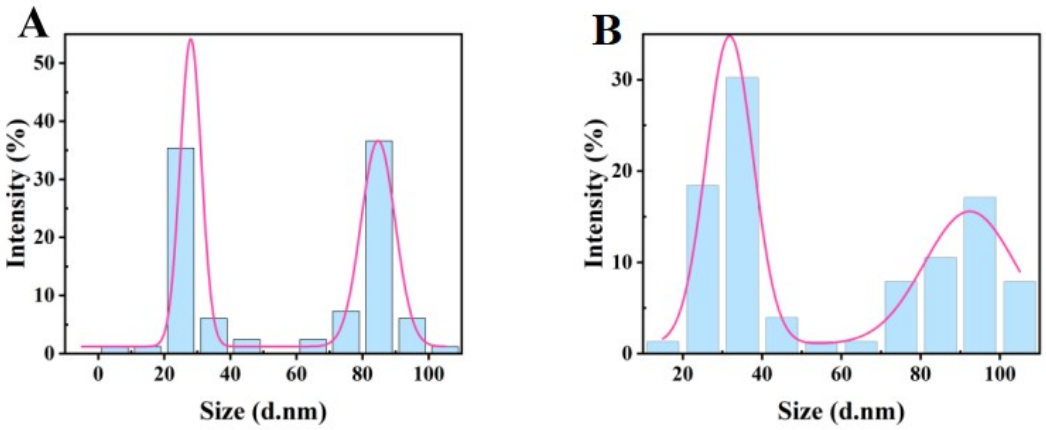

147

148 **Figure S3.** TEM size distributions of AuNBP (A) and AuNBP@ mAb (B).

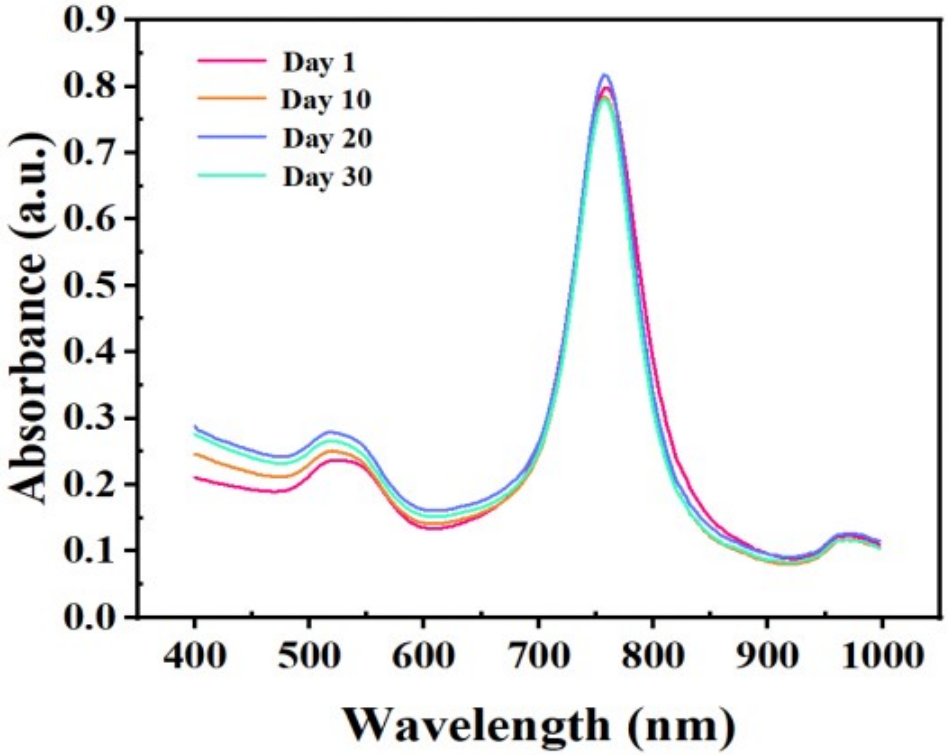

149

150 **Figure S4.** UV-Vis absorption spectra of AuNBP@ mAb during storage.

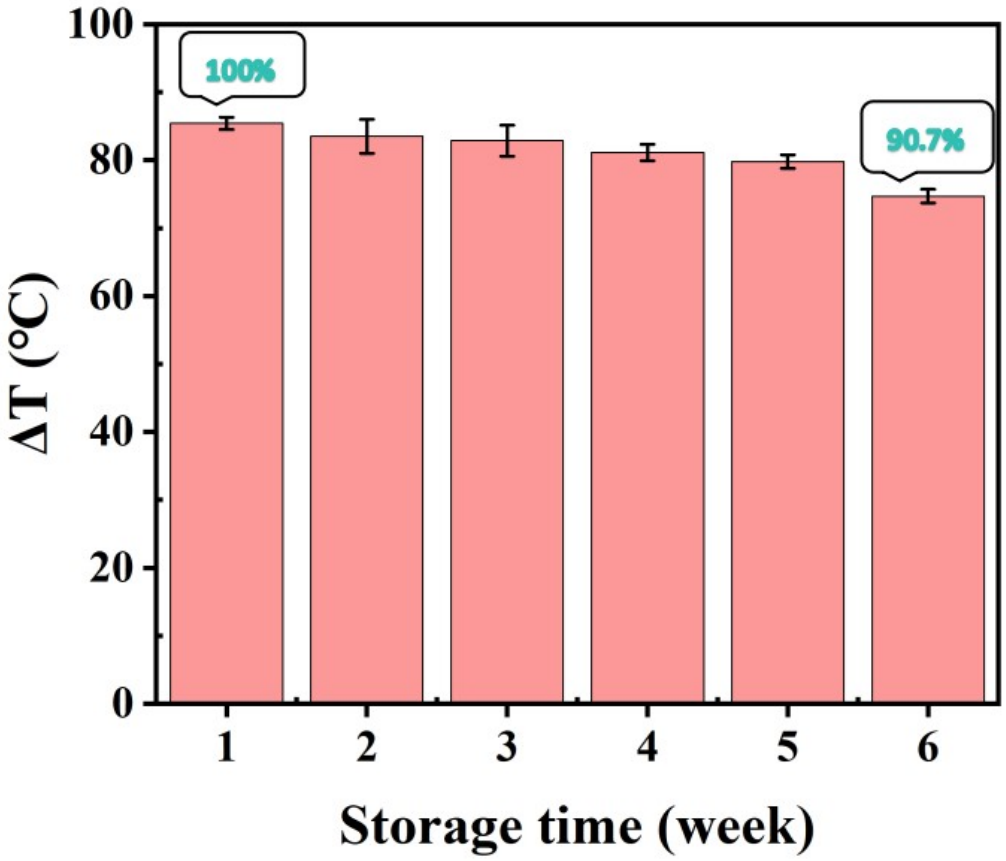

Figure S5. Photothermal signal intensities obtained from detection with AuNBP@mAb probe solution stored at different times.

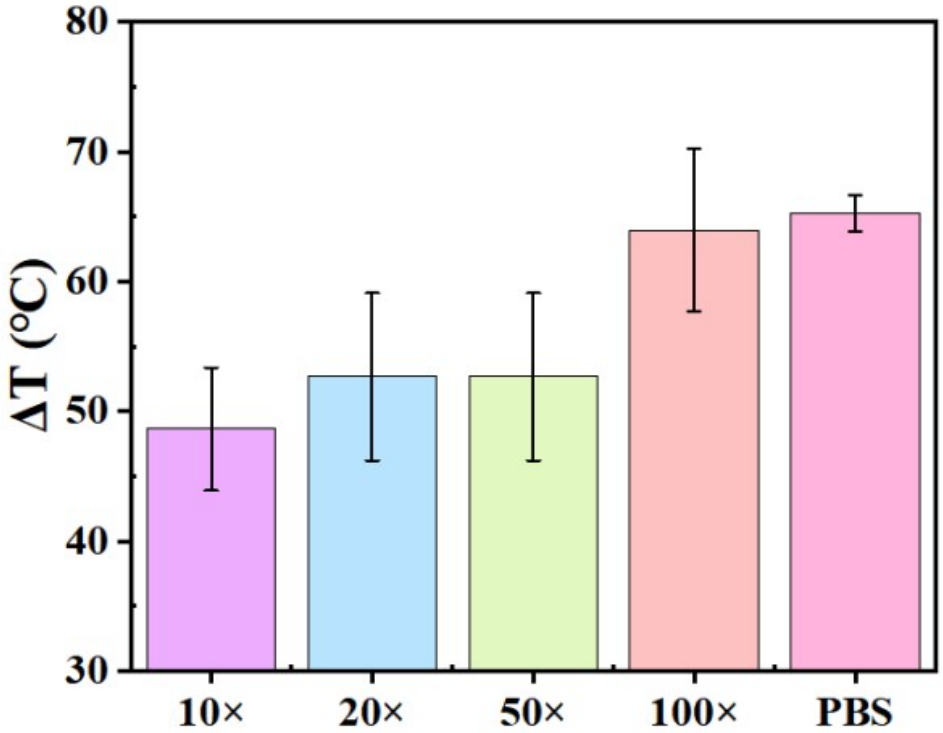

Figure S6. The influence of the dilution time of methanol on the performance of the dual mode LFIA. 10×represents a 10-fold dilution of methanol, 20×represents a 20-fold dilution of methanol, 50×represents a 50-fold dilution of methanol, 100×represents a 100-fold dilution of methanol.

Figure S7. Photograph of our LFIA kits for practical tests. Each LFIA kit contains an assembled strip, a methanol extract (A); a tube of PBST (B); and a tube of probe solution (C).

2. Supporting tables 1-3

Table S1. Comparison of the LOD and detection range of our dual-mode LFIA based on AuNBP with previously reported methods.

Method	Identify the component	Output signal	Detection range (ng/mL)	LOD (ng/mL)	Sample	Reference
LFIA	Monoclonal antibodies	Colorimetric	0.2-211.8	4.8	Citrus fruits	This work
		photothermal	1.18-12.3	3.8		
Radio immunoassay	Polyclonal antibodies	-	-	2.2	Citrus juice	3
ELISA	Polyclonal antibodies	Colorimetric	-	100.0	Citrus juice	4
ELISA	Monoclonal antibodies	Colorimetric	1.25-23.84	5.4	Citrus fruits	1
HPLC	-	UV-Vis absorption detector	250-500	-	Citrus fruits	5
UPLC-MS-MS	-	MS	-	0.0783	Human urine	6
UPLC-MS-MS	-	MS	122.9-622.9	1.02	Wuji pill	7
UPLC-MS	-	MS	-	2.0	Rat plasma	8
UPLC-MS	-	MS	-	＜100	Citrus juice	9

169 **Table S2. Structural analogues of several limonin used in the specificity test.**

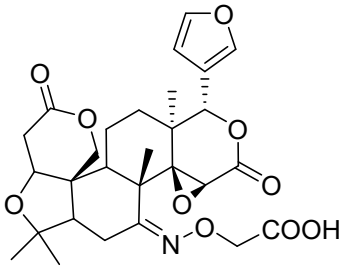	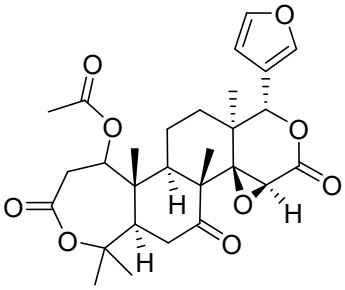
Limonin	**Nomilin**
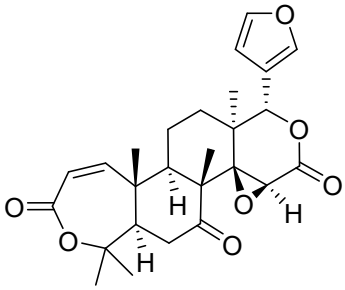	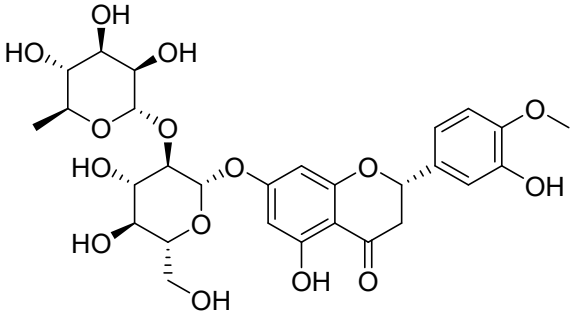
Obacunon	**Neohesperidin**
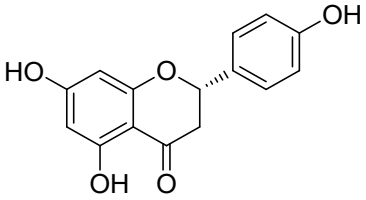	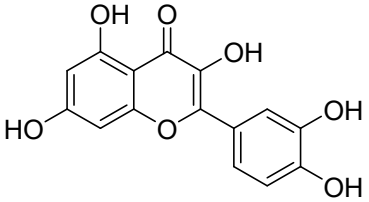
Naringenin	**Quercetin**
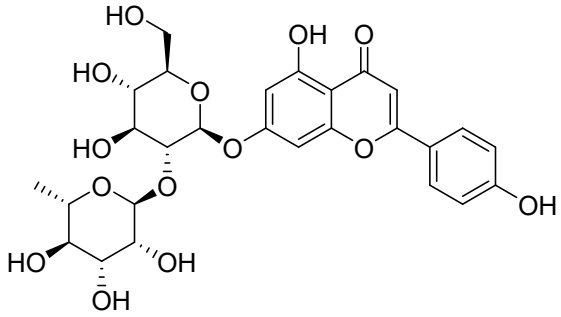	
Rhoifolin	

170

171 **Table S3. Results of intra-assay and inter-assay stability analysis.**

Limonin concentration (ng/mL)	Intra-assay			Inter-assay		
	Mean (°C)	SD (°C)	CV (%)	Mean (°C)	SD (°C)	CV (%)
10	83.4	2.1	2.5	84.7	4.7	5.6
1	111.7	1.8	1.6	104.8	6.5	6.2

172

References:

1. D. Sun, Y. Liu, Z. Jin, B. Xu, Y. Jin, Q. Zhao, Y. He, J. Li, Y. Zhang and Y. Cui, *Food Chemistry*, 2024, **447**, 138989.
2. A. Sánchez-Iglesias, N. Winckelmans, T. Altantzis, S. Bals, M. Grzelczak and L. M. Liz-Marzán, *Journal of the American Chemical Society*, 2016, **139**, 107-110.
3. E. W. Weiler and R. L. Mansell, *J. Agric. Food Chem.*, 1980, **28**, 543-545.
4. P. S. Jourdan, R. L. Mansell, D. G. Oliver and E. W. Weiler, *Anal. Biochem.*, 1984, **138**, 19-24.
5. A. Vikram, G. K. Jayaprakasha and B. S. Patil, *Anal. Chim. Acta*, 2007, **590**, 180-186.
6. S. J. Liu, J. Zhang, L. Zhou, B. Y. Yu, C. Y. Li, Z. X. Liu and W. Z. Ju, *J. Chromatogr. B*, 2012, **907**, 163-167.
7. T. T. Tian, Y. R. Jin, Y. H. Ma, W. W. Xie, H. J. Xu and Y. F. Du, *J. Chromatogr. Sci.*, 2016, **54**, 237-245.
8. J. J. Zhao, X. Han, X. Zhao, C. Wang, Q. Li, X. H. Chen and K. S. Bi, *Anal. Bioanal. Chem.*, 2011, **401**, 289-296.
9. J. E. Young, J. J. Pesek and M. T. Matyska, *Lc Gc North America*, 2015, **33**, 192-199.